Journal of Applied Polymer Science

Preparation, Characterization, Antifungal Activity, and Mechanism of Chitosan/TiO_2 Hybrid Film Against *Bipolaris maydis*

Qunzeng Huang,[1] Zhujin Jiao,[2] Min Li,[3] Dongfang Qiu,[1] Kecheng Liu,[1] Hengzhen Shi[1]

[1]College of Chemistry and Pharmacy Engineering, Nanyang Normal University, Nanyang 473061, People's Republic of China

[2]Henan Province Key Laboratory of Funiu Mountain Insect Biology, Nanyang Normal University, Nanyang 473061, People's Republic of China

[3]Department of Chemistry, Henan Institute of Education, Zhengzhou 450046, People's Republic of China

Correspondence to: H. Shi (E-mail: hzshi@nynu.edu.cn)

ABSTRACT: A chitosan/TiO_2 hybrid film, as a powerful antifungal material for controlling southern corn leaf blight, which is caused by the fungus *Bipolaris maydis* (*B. maydis*), was prepared and characterized. Its antifungal activity toward *B. maydis* was studied, and the experimental results indicate that it had multiple attractive antifungal properties as follows: (1) it displayed strong antifungal activity against *B. maydis*, with an inhibition ratio of 100% under both visible-light irradiation and in a dark environment; (2) it exhibited a superior antifungal efficacy of 100%, even after 4 h under the irradiation of visible light; and (3) its antifungal activity included the effect of hydroxyl radicals generated by the photocatalysis of TiO_2. The antifungal mechanism was attributed to the action of a large amount of positive charges on the structure of the hybrid film, which interacted with the negative charges from the cell and finally resulted in the inactivation of *B. maydis*. © 2012 Wiley Periodicals, Inc. J. Appl. Polym. Sci. 000: 000–000, 2012

KEYWORDS: films; polysaccharides; properties and characterization

Received 25 April 2012; accepted 4 July 2012; published online
DOI: 10.1002/app.38322

INTRODUCTION

Southern corn leaf blight (SCLB), caused by the ascomycetous fungus *Bipolaris maydis* (Nisikado & Miyake) Shoemaker, is a serious disease for maize, which can lead to severe economic losses in agriculture. The spores of *B. maydis* germinate on the leaf surface and infect the host directly. Under favorable conditions, the mycelium of *B. maydis* produces more conidiophores in the daytime. At present, the application of chemical pesticides has been the major strategy for the control of SCLB. However, long-term use of chemical pesticides can cause damage to the environment and to human health. Therefore, it is important to develop ecofriendly materials for the effective management of SCLB.

Chitosan (CS), a linear copolymer of β-(1,4)-linked 2-acetamido-2-deoxy-β-*d*-glycopyranosyl units and 2-amino-2-deoxy-β-*d*-glycopyranosyl units, is readily soluble in dilute acidic solutions below pH 6.0 because of the protonation of the amine groups that have a pK_a value of 6.3. This makes CS a water-soluble cationic polyelectrolyte[1] and confers onto CS numerous and unique chemical, physical, physiological, and biological properties, especially excellent antibacterial, antiviral, and antifungal activities and good film-forming abilities.[2–5] In recent years, CS films have been the focus of intense interest for inhibiting the growth of bacteria.[6–11]

However, as a monocomponent fungicidal agent, CS's narrow antimicrobial range and weak mechanical strength are frequently not sufficient for meeting the requirements of practical applications. The blending of inorganic nanoparticles into the polymer matrix has already proven to be an effective way to enhance the performance of CS films. Most importantly, organic/inorganic hybrid materials fabricated by this method not only share the individual characteristics of both components but also result in new properties. Among many kinds of inorganic nanoparticles, TiO_2 has received considerable attention because of its good chemical stability, nontoxicity, low cost, high photocatalytic activity, and antibacterial properties.[12–16] Particularly, the spread characteristics and modes of *B. maydis* spores are more favorable for taking advantage of the photocatalytic properties of TiO_2 nanoparticles because TiO_2 can produce a highly reactive radical with a highly oxidative and reactive nature under light irradiation. Our previous study indicated that a nitrogen-doped TiO_2 photocatalyst could effectively inhibit the germination of *B. maydis* under visible-light irradiation.[17] In addition, the surface charge properties of TiO_2

depend strongly on the solution pH and its point of zero charge (PZC). At pH < pH at PZC, the TiO_2 particle surface is positively charged, whereas at pH > pH at PZC, the surface is negatively charged; this is described by eqs. (1) and (2):[18,19]

$$Ti^{IV}—OH + H^+ \rightarrow Ti^{IV}—OH_2^+ \quad (pH < pHpzc) \qquad (1)$$

$$Ti^{IV}—OH + H^- \rightarrow Ti^{IV} - O^- + H_2O \quad (pH < pHpzc) \qquad (2)$$

Therefore, a proper pH value below the pH at PZC of TiO_2 and the pK_a of CS will enable both the surface of the TiO_2 nanoparticles and the molecular chain of CS to acquire positive charges. Under the electrostatic repulsion forces between inorganic nanoparticles and the polymer matrix, the flexible chain of CS molecules can be fully stretched out, and the dispersion of nanoparticles in the polymer matrix can be improved; this provides the hybrid film with a larger working area, which carries a positive charge and leads to a better adsorption effect on the spores of *B. maydis*.

On the basis of the previous considerations, we expected to develop a chitosan/TiO_2 hybrid film (CTHF) by controlling the interfacial interactions of TiO_2 nanoparticles with CS polymers to effectively destroy or inhibit the growth of *B. maydis* spores. Until now and as far as we know, there have been few studies on organic/inorganic hybrid films as agricultural fungicides for plant disease control. Consequently, it is very necessary and important to study the effect of interfacial interactions between inorganic nanoparticles and the polymer matrix on the structure and antifungal activity of hybrid films.

In this study, CTHF coated on a glass substrate was prepared by control of the interfacial interactions of TiO_2 nanoparticles with CS polymers. The preparation process of CTHF was optimized by an orthogonal test, and the hybrid film was characterized. The antifungal activity of CTHF toward *B. maydis* was studied for the first time.

EXPERIMENTAL

Materials

CS was obtained from Yuhuan Biology Engineering Corp. (Zhejiang, China) with a degree of deacetylation of 97.4% and a viscosity-average molecular weight of 270,000. TiO_2 (Degussa P25, anatase crystallite size ≈ 25 nm) was purchased from Guangzhou Hualisen Commerce Corp. Terephthalic acid (TA) and other reagents used were analytical grade and were purchased from Nanyang Chemical Agent Corp. (Nanyang, China). The cling film, with a water vapor permeability of 33 ± 40% (g m^{-2}·24 h^{-1}) and an oxygen permeability of 18,500 ± 40% (cm^3 m^{-2}·24 h^{-1}·atm^{-1}).

Table I. Variables Investigated and Their Levels

	Level of each variable		
Variable	1	2	3
A (g)	0.1	0.2	0.3
B (g)	0.02	0.05	0.08
C (mol/L)	0.0125	0.0250	0.0375
D (°C)	120	130	140

Table II. Experimental Arrangement and Test Results

Experiment number	*A*	*B*	*C*	*D*	Inhibition ratio (%)
1	1	1	1	1	38.5
2	1	2	2	2	85.0
3	1	3	3	3	39.4
4	2	1	2	3	29.9
5	2	2	3	1	89.4
6	2	3	1	2	90.8
7	3	1	3	2	83.7
8	3	2	1	3	41.0
9	3	3	2	1	86.3
K_1	162.9	152.1	170.3	214.2	
K_2	210.1	215.4	201.2	259.5	
K_3	211.0	216.5	212.5	110.3	
R	48.1	64.4	42.2	149.2	

Optimization of the Preparation Process of CTHF

The process of preparing CTHF-coated glass substrates was optimized by an orthogonal test. According to the design theory of the orthogonal test, the orthogonal array L_9 (3^4) was selected to arrange the test program. Four controllable variables, the dosage of CS (*A*), the dosage of TiO_2 (*B*), the molar concentration of acetic acid (*C*), and the drying temperature (*D*), were selected for optimization. Three levels of each factor were investigated. The selected factors and levels are listed in Table I. The inhibition ratio of CTHF was measured for the aforementioned factors and levels, and a further orthogonal analysis was carried out. Thus, the inhibition ratio, variance, and range values, *K* and *R*, were calculated (Table II).

The order of influence for each variable was $D > B > A > C$, as shown in Table II. For the variances of *A*, *B*, and *C*, level 3 was the best according to the theory of the orthogonal test, but for *D*, level 2 was the best. However, for the variance of *A*, level 2 was chosen because the value of K_2 was very close to that of K_3. Most importantly, a solution containing a minor amount of CS was favorable for the dispersion of the nanoparticles. Consequently, the optimum level of each variable was $A_2B_3C_3D_2$.

Preparation of the CTHF-Coated Glass Substrate

Under the optimum conditions determined by the orthogonal test, the CTHF-coated glass substrate was fabricated as follows. First, 0.2 g of CS was dissolved in 50 mL of 0.0375 mol/L aqueous acetic acid. A transparent CS solution with a pH value of 3.21 was obtained. Then, 0.08 g of TiO_2 powder was added to the CS solution, and the mixed solution was stirred continuously for 2 h. Subsequently, with the aid of a casting knife, these suspensions were cast onto clean glass slides. The prepared CTHF was dried at room temperature for 24 h and then dried at 130°C for 4 h.

Preparation of the CS Film Coated on the Glass Substrate

An amount of 0.2 g of CS was dissolved in 50 mL of 0.0375 mol/L aqueous acetic acid. A transparent CS solution was obtained. By the same casting process, the individual sample of CS film coated on the glass substrate was prepared.

Preparation of TiO_2 Powder Coated on the Glass Substrate

An amount of 0.08 g of TiO_2 powder was dispersed into 50 mL of 0.0375 mol/L aqueous acetic acid. A suspension of nanoparticles was obtained. By same casting process, an individual sample of TiO_2 powder coated on the glass substrate was prepared.

Characterization of the Materials

Scanning electron microscopy (SEM) of the CTHF and TiO_2 powder coated on the glass substrate was investigated with a FEI Quanta 200 scanning electron microscope at 30 kV. To conveniently characterize other properties, the CS film and CTHF were peeled off the glass substrates and ground into powder. X-ray diffraction (XRD) patterns of the TiO_2, CS film, and CTHF were recorded on a Bruker D8-Advance X-ray powder diffractometer with monochromatized Cu Kα radiation ($\lambda = 1.5418$ Å) in the range $2\theta = 20$–$80°$. Fourier transform infrared (FTIR) spectra of the TiO_2, CS film, and CTHF were obtained by a Nicolet 5700 FTIR spectrometer with KBr pellets. Diffuse reflectance spectroscopy (DRS) of the TiO_2, CS film, and CTHF were recorded on a Lambda-650S UV–vis spectrophotometer equipped with a diffuse reflectance accessory.

Determination Test of the Antifungal Activity against *B. maydis*

A volume of 20 μL of a spore suspension with an approximate concentration of 3×10^4 spores/mL were dropped onto the center of the glass slides coated with CTHF, CS film, and TiO_2 powder, respectively. Then, the glass slides were immediately covered with a layer of cling film to control the humidity and to prevent the spores from floating on the top of the suspension. Subsequently, these glass slides were placed in a growth chamber with a light intensity of 20,000 Lux, a temperature of 28°C, and a relative humidity of 80%. At various periods, the germination of spores was observed through a Nikon TE2000 microscope, and the germination ratio was obtained. Furthermore, the antifungal activity of CTHF in darkness was also measured under the same conditions. The germination and inhibition ratio of the spores were determined with eqs.(3) and (4):

$$\text{Germination ratio } (\%) = \frac{C_g}{C_t} \times 100 \quad (3)$$

$$\text{Inhibition ratio } (\%) = \frac{C_{ug}}{C_t} \times 100 \quad (4)$$

where C_g and C_{ug} are the statistical count of the germinated and ungerminated spores treated with the film samples, respectively, and C_t is the total count of spores.

Determination Test of Hydroxyl Radicals (·OH)

The determination of ·OH was done with a TA fluorescence probe.[20] The measurements of the amount of ·OH were performed as follows: 0.50 g of CTHF was added to an 80-mL

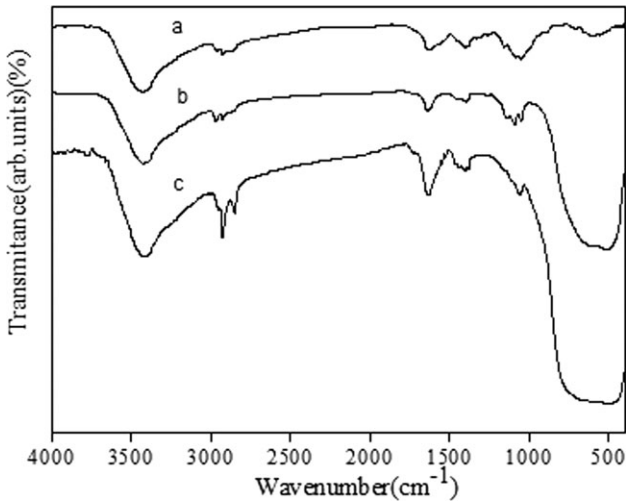

Figure 2. FTIR spectra of the powder of the (a) CS film, (b) TiO_2, and (c) CTHF.

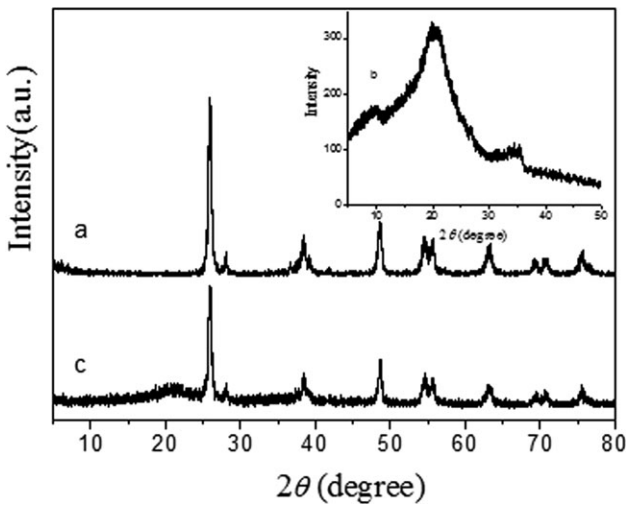

Figure 1. XRD patterns of the powder of the (a) TiO_2, (b) CS film, and (c) CTHF.

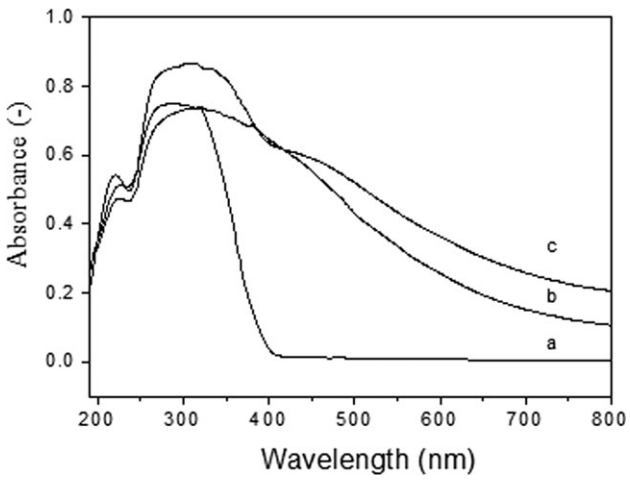

Figure 3. DRS patterns of the powder of (a) TiO_2, (b) CS film, and (c) CTHF.

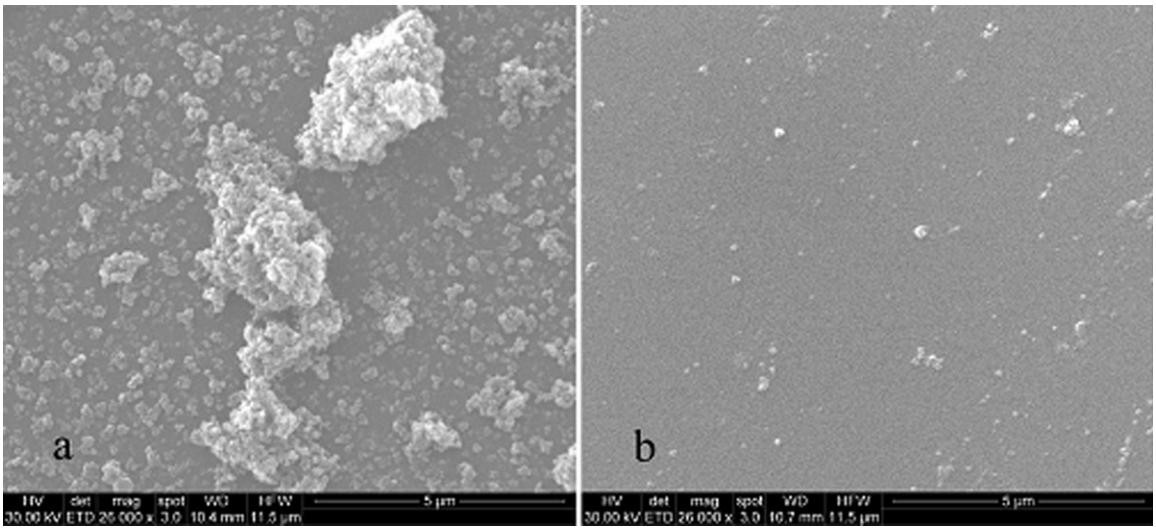

Figure 4. SEM morphology of (a) TiO_2 powder and (b) CTHF coated on a glass slide.

Pyrex quartz glass bottle with 50 mL of aqueous solution containing 0.2 mmol NaOH and 0.05 mmol TA and then irradiated under visible light ($\lambda > 420$ nm) with stirring. At 30, 60, 90, and 120 min, 8 mL suspensions were extracted and centrifuged at a speed of 12,000 rpm. The fluorescence spectra of these supernatant liquids were obtained on a Varian Cary Eclipase fluorescence spectrometer.

RESULTS AND DISCUSSION

Characterization of the Materials

Figure 1 shows the XRD patterns of the TiO_2 powder, powdered CS, and CTHF films. The diffraction peaks of TiO_2 at $2\theta = 25.92$ and 27.94° were attributed to the characteristic peaks of anatase (101) and the rutile (110) crystal phase,[21,22] which was composed of a mixed phase with 95% anatase and 5% rutile [Figure 1(a)]. The powder of the CS film showed characteristic peaks at $2\theta = 9.71$ and 20.38°, which were assigned to (020) and (100) reflections[23,24] [Figure 1(b)]. As expected, the powder of CTHF exhibited the typical characterization peaks of TiO_2; this indicated that the existence of CS had no effect on the crystalline structure of TiO_2 and that the introduction of TiO_2 particles into the CS phase resulted in the disappearance of the peak at $2\theta = 9.71°$ and an intensity decrease of the peak at $2\theta = 20.38°$ [Figure 1(c)]. It was hypothesized that TiO_2 particles interfered with the ordered packing of polymer chains by hydrogen bonding, which led to the decrease in the CS crystallinity.[25]

FTIR spectra for the powders of the CS film, TiO_2, and CTHF are presented in Figure 2. The absorption bands of CS at 1044 and 3422 cm^{-1} were assigned to the stretching vibrations of —OH groups, and the band at 1630 cm^{-1} was attributed to the bending vibrations of —NH_2 groups.[25,26] The peaks of TiO_2 at 1093, 2851, and 3429 cm^{-1} were ascribed to surface hydroxyl groups and adsorbed water molecules,[27,28] and the band at 455–760 cm^{-1} corresponded to the Ti—O—Ti stretching vibration mode.[28,29] In comparison with the FTIR spectra of the individual CS and TiO_2, CTHF exhibited most of the characteristic adsorption peaks of CS and TiO_2 but displayed some slight changes in the intensity of the peaks assigned to the amino and hydroxyl groups of CS and the surface hydroxyl groups of TiO_2. These changes were relevant to the formation of hydrogen bonds between the —OH or —NH_2 groups of CS or —OH groups on the surface of the TiO_2 nanoparticles.

Figure 3 shows the DRS spectra of the powders of the CS film, TiO_2, and CTHF. CS had two strong absorption bands at 220 and 320 nm, which corresponded to the $n \rightarrow \sigma^*$ transition of amido groups and the $n \rightarrow \pi^*$ transition of carbonyl groups, respectively.[30] Obviously, the absorption edge of CTHF displayed a significant redshift and response in the visible region. The redshift might have been caused by the combination between the TiO_2 particles and CS through hydrogen bonding.[31]

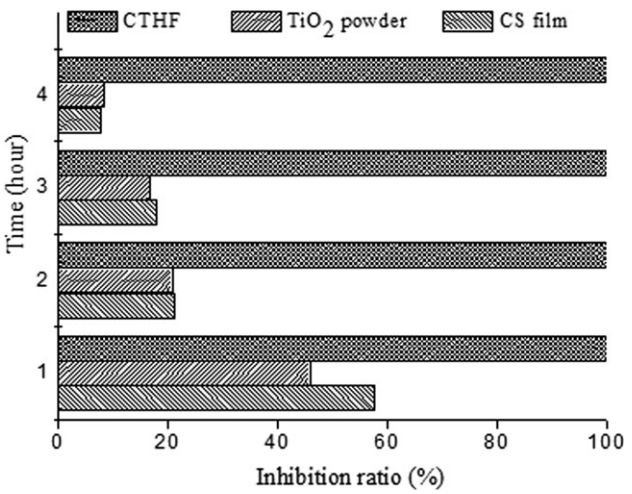

Figure 5. Effect of the irradiation time on the inhibition ratio of *B. maydis* spores treated with CTHF, CS film, and TiO_2 powder coated on a glass slide.

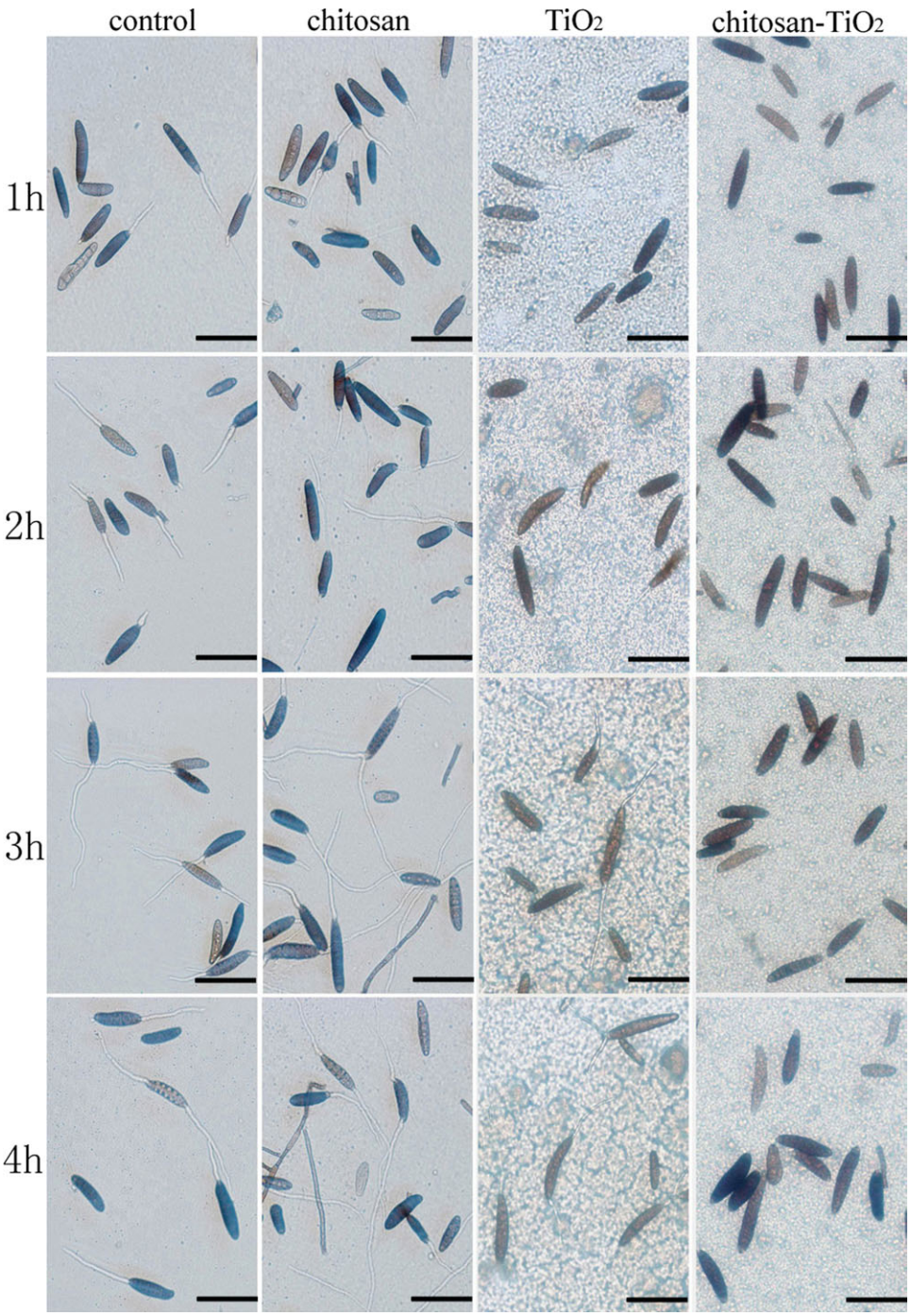

Figure 6. Microscopy photographs of *B. maydis* spores at different intervals after they were treated with the control, CTHF, CS film, and TiO_2 powder coated on a glass slide (bar = 300 μm). [Color figure can be viewed in the online issue, which is available at www.interscience.wiley.com.]

The SEM photographs of the CTHF film and TiO_2 powder are shown in Figure 4. The agglomeration of the nanoparticles, shown in Figure 4(a), was apparent, and the surface was rough, but that in Figure 4(b) was more uniform and smoother on the same scale. The results confirm that the electrostatic repulsive forces between the polymer chains of CS and the surface of the TiO_2 nanoparticles played a major role in breaking down the undesirable agglomeration of inorganic nanoparticles.

Antifungal Activity

The antifungal effects evaluated on *B. maydis* of the CS film, CTHF, and TiO_2 powder coated on glass slides and sterile water as a control were examined under visible-light irradiation for 1, 2, 3, and 4 h, respectively. The experimental results show that CTHF had outstanding antifungal activity against *B. maydis*, with an inhibition ratio of 100% at different intervals, compared with those of the individual CS film and TiO_2 powder

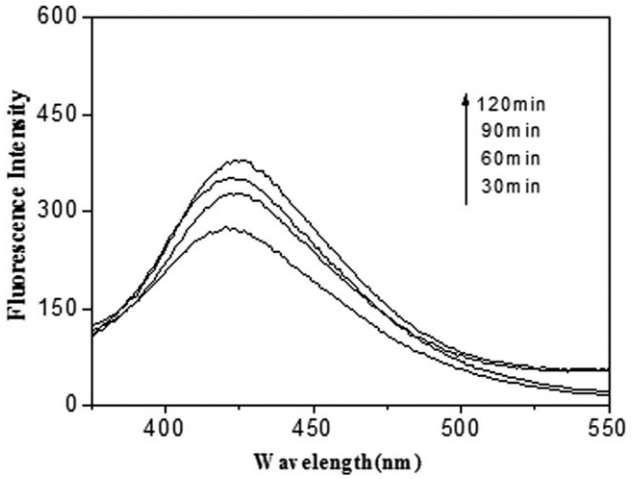

Figure 7. Fluorescence spectra at various periods that were obtained from the supernatant liquid of the irradiated CTHF on the excitation of 312 nm.

coated on glass slides. As shown in Figure 5, the CS film and TiO_2 powder had inhibition ratios of 57.7 and 45.9% at 1 h, respectively, but the inhibition ratio decreased gradually with increasing irradiation time and was even down to 7.8 and 8.3% at 4 h, respectively. Surprisingly, CTHF had a strong and stable inhibition effect on the growth of *B. maydis* spores; this indicated a notable synergistic effect. It should be pointed out that the influence of acetic acid used in the preparation procedure of the film could be ignored according to the antifungal results of the CS film. Furthermore, a *D* of 130°C could quickly evaporate acetic acid with a boiling point of 118°C.

The morphology of *B. maydis* spores treated with the CTHF, CS film, and TiO_2 powder coated on glass slides and sterile physiological water as control were examined under light microscopy, and the microscopic observations of the course of germination are shown in Figure 6. As shown in these photos, in which *B. maydis* spores were treated with sterile physiological water, for the individual CS film and TiO_2 powder, the spores germinated unceasingly, and a germ tube gradually formed with increasing time. Although both the CS film and TiO_2 powder had inhibitory ability, the effect was weaker compared with that of CTHF because of the low-mass concentration of CS and the intrinsic properties of TiO_2. In addition and extremely interestingly, CTHF had the same effect on inhibiting the germination of spores at the same interval in darkness. The photos of the antifungal activities in darkness were not put in Figure 6 because they showed the same experimental results as those under the irradiation conditions.

Antifungal Mechanism

To confirm whether the wonderful antifungal capacity of CTHF was based on hydroxyl radicals produced by photocatalysis, a determination test of ·OH was designed by a TA fluorescence probe. Figure 7 shows the fluorescence spectra of TAOH generated from TA by the reaction with ·OH. As shown in Figure 7, an obvious and strong fluorescent emission at 423 nm was observed under visible-light irradiation. Moreover, the fluorescence intensity increased linearly against time.

The fact that the hydroxyl radical was produced by the photocatalysis of TiO_2 under visible-light irradiation seemed to imply that the antifungal capacity of CTHF was related to the photocatalytic properties of TiO_2. However, on the basis of the experimental phenomena that CTHF could completely inhibit the growth of *B. maydis* in darkness, we speculated that the antifungal activity of CTHF against *B. maydis* might have been closely related to its particular structure, instead of being simply due to the photocatalytic properties of TiO_2.

The analyses results of XRD, FTIR spectroscopy, DRS, and SEM indicated that the interfacial interaction of TiO_2 with CS had a strong influence on the structure of CTHF. On the one hand, the surface of TiO_2 and the molecular chain of CS were positively charged, as deduced from the pH value of the reaction system and the PZC value (6.8 ± 0.2)[32] of standard Degussa P25 material. Then, the effect of the electrostatic repulsion force resulted in the molecular chains of CS being stretched out at the maximum limit, and the dispersion of nanoparticles in polymer matrix was improved, which helped to break down the undesirable agglomeration of inorganic nanoparticles. On the other hand, CS carried a large number of amino and hydroxyl groups; this was suitable for the formation of hydrogen bonds by the interactions with the surface hydroxyls of TiO_2. The interfacial interactions of electrostatic repulsion and hydrogen bonding were advantageous for hybrid film formation to obtain a stable openwork structure that carried large amounts of positive charges. Subsequently, these positive charges on the structure played a very important role in inhibiting the growth of *B. maydis* spores, which were negatively charged; this may have interfered with the nutrient exchange between the exterior and interior of the cell and finally resulted in halted pathogen growth.[33–35] Of course, the excellent antifungal activity of CTHF against *B. maydis* under visible-light irradiation may have also been attributed to the hydroxyl radical produced from photocatalysis in addition to the decisive influence of structural factors.

CONCLUSIONS

In this study, we were concerned with the antifungal activity of CTHF developed by controlling the interfacial interactions between TiO_2 nanoparticles and CS polymers. We observed that the hybrid film completely inhibited the germination of *B. maydis* in visible-light and dark environment. These research results not only offer a kind of environmental protection material for treating *B. maydis* fungi but also opens up a new way for emboldening and applying natural CS.

ACKNOWLEDGMENTS

This study was financially supported by the National Natural Science Foundation of China (project number 20943003).

REFERENCES

1. Dash, M.; Chiellini, F.; Ottenbrite, R. M.; Chiellini, E. *Prog. Polym. Sci.* **2011,** *36*, 981.
2. Bautista-Baños, S.; Hernández-Lauzardo, A. N.; Velázquez-del Valle, M. G.; Hernández-Lópeza, M.; Ait Barka, E.; Bosquez- Molinac, E.; Wilson, C. L. *Crop Prot.* **2006,** *25*, 108.

3. Hadrami, A. E.; Adam, L. R.; Hadrami, I. E.; Daayf, F. *Mar. Drugs* **2010,** *8*, 968.
4. Rabea, E. I.; Badawy, M. E. T.; Stevens, C. V.; Smagghe, G.; Steurbaut, W. *Biomacromolecules* **2003,** *4*, 1457.
5. Kumar, M. N. V. R.; Muzzarelli, R. A. A.; Muzzarelli, C.; Sashiwa, H.; Domb, A. *J. Chem. Rev.* **2004,** *104*, 6017.
6. Chen, M. C.; Yeh, G. H. C.; Chiang, B. H. *J. Food Process. Pres.* **1996,** *20*, 279.
7. Coma, V.; Martial-Gros, A.; Garreau, S.; Copinet, A.; Deschamps, A. *J. Food Sci.* **2002,** *67*, 1162.
8. Ouattara, B.; Simard, R. E.; Piette, G.; Begin, A.; Holley, R. A. *J. Food Sci.* **2000,** *65*, 768.
9. Khalid, Z.; Idoya, F. P.; Maite, R.; Juan, I. M. *Food Hydrocolloids* **2009,** *23*, 2309.
10. Martinez, A. P.; Cortez, M. O.; Ezquerra, J. M.; Graciano, A. Z.; Rodriguez, F.; Castillo, M. M.; Yepiz, M. S.; Plascencia, M. *Carbohydr. Polym.* **2010,** *82*, 305.
11. Sebti, I.; Martial-Gros, A.; Carnet-Pantiez, A.; Grelier, S.; Coma, V. *J. Food Sci.* **2005,** *70*, 100.
12. Kikuchi, Y.; Sunada, K.; Iyoda, T.; Hashimoto, K.; Fujishima, A. *J. Photochem. Photobiol. A* **1997,** *106*, 51.
13. Liu, H. L.; Yang, T. C. K. *Process. Biochem.* **2003,** *39*, 475.
14. Peng, C. C.; Yang, M. H.; Chiu, W. T.; Chiu, C. H.; Yang, C. S.; Chen, Y. W.; Chen, K. C.; Peng, R. Y. *Macromol. Biosci.* **2008,** *8*, 316.
15. Qian, T. T.; Su, H. J.; Tan, T. W. *J. Photochem. Photobiol. A* **2011,** *218*, 130.
16. Yuan, W. Y.; Ji, J.; Fu, J. H.; Shen, J. C. *J. Biomed. Mater. Res. B* **2008,** *85*, 556.
17. Li, M.; Huang, Q. Z.; Qiu, D. F.; Jiao, Z. J.; Meng, Z. H.; Shi, H. Z. *Chin. Chem. Lett.* **2010,** *21*, 117.
18. Dutta, P. K.; Ray, A. K.; Sharma, V. K.; Millero, F. J. *J. Colloid Interface Sci.* **2004,** *278*, 270.
19. Rodriguez, P.; Meille, V.; Pallier, S.; Sawah, M. A. A. *Appl. Catal. A* **2009,** *360*, 154.
20. Xiao, Q.; Ouyang, L. L. *Chem. Eng. J.* **2009,** *148*, 248.
21. Jing, L. Q.; Xin, B. F.; Yuan, F. L. *J. Phys. Chem. B.* **2006,** *110*, 17860.
22. Zhang, Q. H.; Gao, L.; Guo, J. K. *Appl. Catal. B* **2000,** *26*, 207.
23. Kim, J. H.; Lee, Y. M. *Polymer* **1993,** *34*, 1952.
24. Tian, F.; Liu, Y.; Hu, K.; Zhao, B. Y. *J. Mater. Sci.* **2003,** *38*, 4709.
25. Yang, D.; Li, J.; Jiang, Z. Y.; Lu, L. Y.; Chen, X. *Chem. Eng. Sci.* **2009,** *64*, 3130.
26. Khan, R.; Dhayal, M. *Electrochem. Commun.* **2008,** *10*, 492.
27. Ding, Z.; Lu, G. Q.; Greenfield, P. F. *J. Phys. Chem. B.* **2000,** *104*, 4815.
28. Jing, L. Q.; Fu, H. G.; Wang, B. Q.; Wang, D. J.; Xin, B. F.; Li, S. D.; Sun, J. Z. *Appl. Catal. B* **2006,** *62*, 282.
29. Sigaev, V. N.; Pernice, P.; Aronne, A.; Akimova, O. V.; Stefanovich, S. Y.; Scaglione, A. *J. Non-Cryst. Solids* **1990,** *126*, 202.
30. Wang, S. M.; Huang, Q. Z.; Wang, Q. S. *Carbohydr. Res.* **2005,** *340*, 1143.
31. Zhang, X.; Su, H.; Zhao, Y.; Tan, T. W. *J. Photochem. Photobiol. A* **2008,** *199*, 123.
32. Fernandez-Ibanez, P.; Nieves, F. J. D. L.; Malato, S. *J. Colloid Interface Sci.* **2000,** *227*, 510.
33. Ben-Shalom, N.; Ardi, R.; Pinto, R.; Aki, C.; Fallik, E. *Crop Protect.* **2003,** *22*, 285.
34. Meng, X. H.; Li, B. Q.; Liu, J.; Tian, S. P. *Food Chem.* **2008,** *106*, 501.
35. Xu, J. G.; Zhao, X. M.; Han, X. W.; Du, Y. G. *Pestic. Biochem. Physiol.* **2007,** *87*, 220.